Long Noncoding RNA HOXA11-AS Modulates the Resistance of Nasopharyngeal Carcinoma Cells to Cisplatin via miR-454-3p/c-Met

Feng-Jie Lin[1,4], Xian-Dong Lin[2,4], Lu-Ying Xu[1], and Shi-Quan Zhu[3,*]

[1]Department of Head & Neck Radiation Oncology, Fujian Cancer Hospital & Fujian Medical University Cancer Hospital, Fuzhou 350014, China, [2]Laboratory of Radiation Oncology and Radiobiology, Fujian Cancer Hospital & Fujian Medical University Cancer Hospital, Fuzhou 350014, China, [3]Department of Pharmacy, Fujian Cancer Hospital & Fujian Medical University Cancer Hospital, Fuzhou 350014, China, [4]These authors contributed equally to this work.
*Correspondence: zsq@fjzlhospital.com
https://doi.org/10.14348/molcells.2020.0133
www.molcells.org

To elucidate the mechanism of action of HOXA11-AS in modulating the cisplatin resistance of nasopharyngeal carcinoma (NPC) cells, HOXA11-AS and miR-454-3p expression in NPC tissue and cisplatin-resistant NPC cells were measured via quantitative reverse transcriptase polymerase chain reaction. NPC parental cells (C666-1 and HNE1) and cisplatin-resistant cells (C666-1/DDP and HNE1/DDP) were transfected and divided into different groups, after which the MTT method was used to determine the inhibitory concentration 50 (IC_{50}) of cells treated with different concentrations of cisplatin. Additionally, a clone formation assay, flow cytometry and Western blotting were used to detect DDP-induced changes. Thereafter, xenograft mouse models were constructed to verify the *in vitro* results. Obviously elevated HOXA11-AS and reduced miR-454-3p were found in NPC tissue and cisplatin-resistant NPC cells. Compared to the control cells, cells in the si-HOXA11-AS group showed sharp decreases in cell viability and IC_{50}, and these results were reversed in the miR-454-3p inhibitor group. Furthermore, HOXA11-AS targeted miR-454-3p, which further targeted c-Met. In comparison with cells in the control group, HNE1/DDP and C666-1/DDP cells in the si-HOXA11-AS group demonstrated fewer colonies, with an increase in the apoptotic rate, while the expression levels of c-Met, p-Akt/Akt and p-mTOR/mTOR decreased. Moreover, the si-HOXA11-AS-induced enhancement in sensitivity to cisplatin was abolished by miR-454-3p inhibitor transfection. The *in vivo* experiment showed that DDP in combination with si-HOXA11-AS treatment could inhibit the growth of xenograft tumors. Silencing HOXA11-AS can inhibit the c-Met/AKT/mTOR pathway by specifically upregulating miR-454-3p, thus promoting cell apoptosis and enhancing the sensitivity of cisplatin-resistant NPC cells to cisplatin.

Keywords: cisplatin, c-Met, drug resistance, HOXA11-AS, miR-454-3p, nasopharyngeal carcinoma

INTRODUCTION

Nasopharyngeal carcinoma (NPC), a highly malignant nasopharyngeal mucosal epithelial tumor, has become the most common head and neck malignant tumor and is characterized by strong infiltration and susceptibility to distant metastasis, which (Jia and Qin, 2012). Principally, the clinical treatment for NPC is carried out through radiotherapy, chemotherapy and surgery (Zhang et al., 2013). In particular, for mid-term or advanced NPC, a combination of chemotherapy

and radiotherapy is often used to improve the therapeutic effect (Kamran et al., 2015). However, these strategies do little to increase the survival of patients after treatment, with a 5-year survival rate of 55% to 60% (Colaco et al., 2013). To date, cisplatin (also known as DDP) in combination with 5-fluorouracil prevails in chemotherapy protocols (Kong et al., 2015), whereas the resistance of tumor cells to DDP that has emerged from chemotherapy is a major cause of treatment failure (Chen et al., 2011). Thus, it is important to explore the resistance of NPC cells to DDP for improving the treatment of NPC.

Long noncoding RNA (lncRNA) represents a group of noncoding RNAs with a length of more than 200 nucleotides (nt) (Han et al., 2016). LncRNA, as reported, can act as competing endogenous RNA (ceRNA) to compete with response elements for binding to the same miRNA, thereby modulating miRNA-targeted genes and playing a key role in tumorigenesis (Song et al., 2018). LncRNA HOXA11-AS, as a member of the homeobox (HOX) family, is a lncRNA with a length of 3885 nt located on chromosome 7p15.2 (Zhang et al., 2016). Recently, investigations have revealed abnormal HOXA11-AS expression in human non-small cell lung cancer (Zhang et al., 2017), gastric cancer (Liu et al., 2017), colorectal cancer (Li et al., 2016), and liver cancer (Yu et al., 2017), as well as its intimate associations with tumor progression and prognosis. More importantly, the work of Zhang et al. (2019) discovered the upregulation of HOXA11-AS in a drug-resistant lung cancer cell and that knockout of HOXA11-AS reversed the resistance of the lung cancer cells to cisplatin. As stated by Zhao et al. (2018), HOXA11-AS can also act as a ceRNA to regulate the expression of miR-454-3p/STAT3 to promote cisplatin resistance of lung adenocarcinoma cells. Through the online miRNA target prediction databases StarBase (http://starbase.sysu.edu.cn) and TargetScan (http://www.targetscan.org), miR-454-3p was identified as having binding sites for HOXA11-AS and c-Met. Zhao et al. (2018) found that approximately 30 miRNAs could sponge with HOXA11-AS, but only miR-454-3p could be observably affected by silenced HOXA11-AS. More importantly, miR-454-3p has been reported to be dysregulated and to function as an oncogene or an anti-oncogene in various tumors (Fang et al., 2015; Zhou et al., 2016). Niu et al. (2015) demonstrated that ectopic miR-454 expression resulted in the inhibition of osteosarcoma cell proliferation and invasion by directly targeting c-Met. As per the evidence of Li et al. (2011), c-Met overexpression has been reported in NPC, while silencing c-Met was shown to abolish the proliferation, invasion and migration of NPC cells. However, little is known about the function and the underlying mechanism of HOXA11-AS and miR-454-3p in NPC.

To solve this problem, we conducted experiments to investigate whether HOXA11-AS can modulate the cisplatin resistance of NPC cells, with the aim to provide a new therapeutic target for NPC treatment.

MATERIALS AND METHODS

Ethical statement
This study was approved by the ethical committee of Fujian Provincial Cancer Hospital (No. 2017-042-01). All patients signed written informed consents to authorize the collection of tissue specimens, and the protocols relating to the animals were approved by the ethical committee for experimental animals of Fujian Cancer Hospital & Fujian Medical University Cancer Hospital. Treatment of the experimental animals was carried out in accordance with the *Guide for the Care and Use of Laboratory Animals* of the National Institutes of Health (Bayne, 1996).

Subjects
Between June 2017 and June 2019, we enrolled 96 NPC patients at our hospital, including 62 males and 34 females with the average age of 58.15 ± 11.23 years (age range, 36-73 years). All patients underwent a biopsy for a nasopharyngeal tumor and were accordingly diagnosed with primary NPC as per the pathological test. Simultaneously, tumor-adjacent tissues were collected and confirmed as normal nasopharyngeal mucosa by a pathological test. All tissue samples were preserved at −80°C following snap freezing in liquid nitrogen.

Cell culture
Cisplatin-sensitive NPC cell lines (C666-1 and HNE1) and their cisplatin-resistant clones (C666-1/DDP and HNE1/DDP) were purchased from the Cell Bank of Xiangya School of Medicine, Central South University. The cells were cultured in RPMI 1640 medium supplemented with 10% inactivated fetal bovine serum (FBS) and 100 µg/ml penicillin and streptomycin, while in the medium for the HNE1/DDP and C666-1/DDP cells, DDP was added at a concentration of 1 µg/ml to sustain the resistance of the cells to DDP, which was removed at 24 h prior to the experiment by replacing the medium with RPMI 1640 medium supplemented only with 10% FBS.

Quantitative reverse transcriptase polymerase chain reaction (qRT-PCR)
TRIzol reagent (Invitrogen, USA) was used to extract total RNA from tissue specimens and cells and was later subjected to determination of the RNA concentration and purity by using a NanoDrop 2000 (Thermo Fisher Scientific, USA) spectrometer. Subsequently, cDNA was prepared from 1 µg of total RNA by using the Reverse Transcription System Kit, and based on the gene sequences in the GenBank database, primers for PCR were designed in Primer 5.0 software (Premier Biosoft International, USA; primer sequences are shown in Table 1). All primers were synthesized by Shanghai Gene-

Table 1. Primer sequences used in qRT-PCR

Gene		Primers
HOXA11-AS	Forward	5'-ACGCTAGGCACCACTTTGTT-3'
	Reverse	5'-CCGGCTACTAGTCAGTGTG-3'
GAPDH	Forward	5'-CCCACTCCTCCACCTTTGAC-3'
	Reverse	5'-GGATCTCGCTCCTGGAAGATG-3'
miR-454-3p	Forward	5'-TAGTGCAATATTGCTTA-3'
	Reverse	5'-CAGTGCGTGTCGTGGAGT-3'
U6	Forward	5'-CTCGCTTCGGCAGCACA-3'
	Reverse	5'-AACGCTTCACGAATTTGCGT-3'

Pharma (China), and the PCRs were all carried out in the ABI PRISM 7500 Real-time PCR System (Applied Biosystem, USA). The relative expression of target genes was quantified via the formula of $2^{-\triangle\triangle Ct}$, with U6 as the internal reference for miR-454-3p and GAPDH as the internal reference for HOXA11-AS, where $\triangle Ct = CT_{\text{target gene}} - CT_{\text{reference gene}}$ and $\triangle\triangle Ct = \triangle Ct_{\text{treatment}} - \triangle Ct_{\text{control}}$.

Cell transfection

Cells in the logarithmic growth phase were plated into a 6-well plate containing complete medium. When the cells reached 80% confluency, cell transfection was performed using the Lipofectamine 2000 Kit (Invitrogen) according to the manufacturer's instructions. The cells were divided into the control group, si-NC group, si-HOXA11-AS group, miR-454-3p inhibitor group, miR-454-3p mimic group, si-c-Met group, si-HOXA11-AS + miR-454-3p inhibitor group and miR-454-3p inhibitor + si-c-Met group, wherein NC siRNA, HOXA11-AS siRNA, miR-454-3p inhibitor, miR-454-3p mimic and c-Met siRNA were all provided by the Shanghai GenePharma.

Dual luciferase reporter assay

HOXA11-AS/c-Met, harboring the binding site of miR-454-3p and HOXA11-AS-WT/c-Met-WT, and HOXA11-AS-MUT/c-Met-MUT, harboring the 3'UTR sequence carrying mutated binding sites, were constructed. HNE1 and C666-1 cells were plated in a 24-well plate, and when the cells reached 80% confluency, the miR-454-3p mimic/miR-454-3p inhibitor/miR-NC (Shanghai GenePharma) and luciferase reporter vector were then cotransfected into the cells by using Lipofectamine 2000 (Invitrogen). After 24 h of transfection, the luciferase reporter gene assay kit (Promega, USA) was utilized to determine the luciferase activity of the cells, which was represented by the ratio of firefly luciferase activity to that of Renilla luciferase activity.

RNA immunoprecipitation

The EZMagna RNA immunoprecipitation (RIP) Kit (Millipore, USA) was used according to the manufacturer's protocol. HNE1 and C666-1 cells were lysed and incubated with RIPA buffer containing magnetic beads conjugated with a human anti-Argonaute2 (Ago2) antibody (Millipore). Normal mouse IgG (Millipore) was used as a negative control. The samples were incubated with proteinase K, after which immunoprecipitated RNA was extracted. Purified RNA was subjected to qRT-PCR analysis.

RNA pull-down assays

The interactions between HOXA11-AS and miR-454-3p, miR-454-3p and c-Met were further examined by RNA pull-down. HOXA11-AS and miR-454-3p were transcribed using T7 RNA polymerase, purified using the RNeasy Plus Mini Kit (Qiagen, Germany), and treated with RNase-free DNase I (Qiagen). Transcribed RNAs were biotin-labeled with the Biotin RNA Labeling Mix. Positive, negative, and biotinylated RNAs were mixed and incubated with HNE1 and C666-1 cell lysates. Magnetic beads were added to each binding reaction, followed by incubation at room temperature. The beads were washed with washing buffer, and qRT-PCR was used to de-

termine the enrichment of the retrieved RNA.

MTT (3-[4,5-dimethylthiazol-2-yl]-2,5 diphenyl tetrazolium bromide) assay

The cells were plated into a 96-well plate, with 2×10^3 cells in each well, followed by incubation at 5% CO_2, saturated humidity and 37°C. Twenty-four hours later, the cells were subjected to treatment with DDP at varying concentrations (0, 2, 4, 8, 16, and 32 μg/ml). After 48 h of culture, MTT reagent (5 mg/ml) was added (20 μl/well) for incubation at 37°C for 4 h. The cells were incubated with 150 μl dimethyl sulfoxide (DMSO) for 30 min. The viability and inhibitory concentration 50 (IC_{50}) value of the cells were calculated based on the readings of each well at a wavelength of 570 nm.

Clone formation assay

HNE1/DDP and C666-1/DDP cells in a logarithmic phase were seeded in a 6-well plate at density of 500-1,000 cells/well, with 3 replicates for each group, and cultured in the complete medium supplemented with 30% FBS and 4 μg/ml DDP. During 7 to 14 days of culture, the medium was refreshed every 3 days to observe the status of the cells under the microscope, including the size of the clone, and the clones that were contained within the microscopic field of vision were photographed. The plate with the cells was then taken out of the incubator, the medium was discarded, and the cells were rinsed in PBS and fixed in 4% paraformaldehyde for 20 min. The cells were then stained in 0.2% crystal violet for 5 min, rinsed in water and dried for photographing. This experiment was repeated three times.

Flow cytometry

HNE1/DDP and C666-1/DDP cells were collected from all groups and seeded in a 6-well plate. In each well, DDP (4 μg/ml) was added, and after 48 h, the cells were collected and digested in 0.25% trypsin, followed by the centrifugation at 2500 rpm for 10 min. Thereafter, the supernatant was discarded; the while the pellet was transferred into a 1.5 ml EP tube and resuspended in 1 ml PBS for 5 min. The cell suspension (100 μl) was placed into tubes with 5 μl fluorescence-labeled annexin V/FITC and 10 μl propidium iodide (20 μg/ml), followed by 15 min of incubation without light. Thereafter, the mixture was mixed with 400 μl staining buffer and then loaded on a flow cytometer (BD Biosciences, USA) for analysis. For each test, 10^4 cells were loaded, and data analysis was performed by using Cell Quest software (BD Biosciences).

Western blotting

The total protein was extracted from cells and subjected to measurement of the protein concentration by using a bicinchoninic acid kit (Boster, China). The proteins were then boiled with loading buffer for 10 min at 95°C, and 50 μg proteins were loaded in each lane of the gel for 10% sodium dodecyl sulfate-polyacrylamide gel electrophoresis (SDS-PAGE) to separate the proteins, which were later transferred onto a polyvinylidene fluoride (PVDF) membrane. The unoccupied sites on the membrane were blocked in 5% bull serum albumin for 1 h. Thereafter, the proteins on the membrane were incubated with primary antibodies to the following proteins
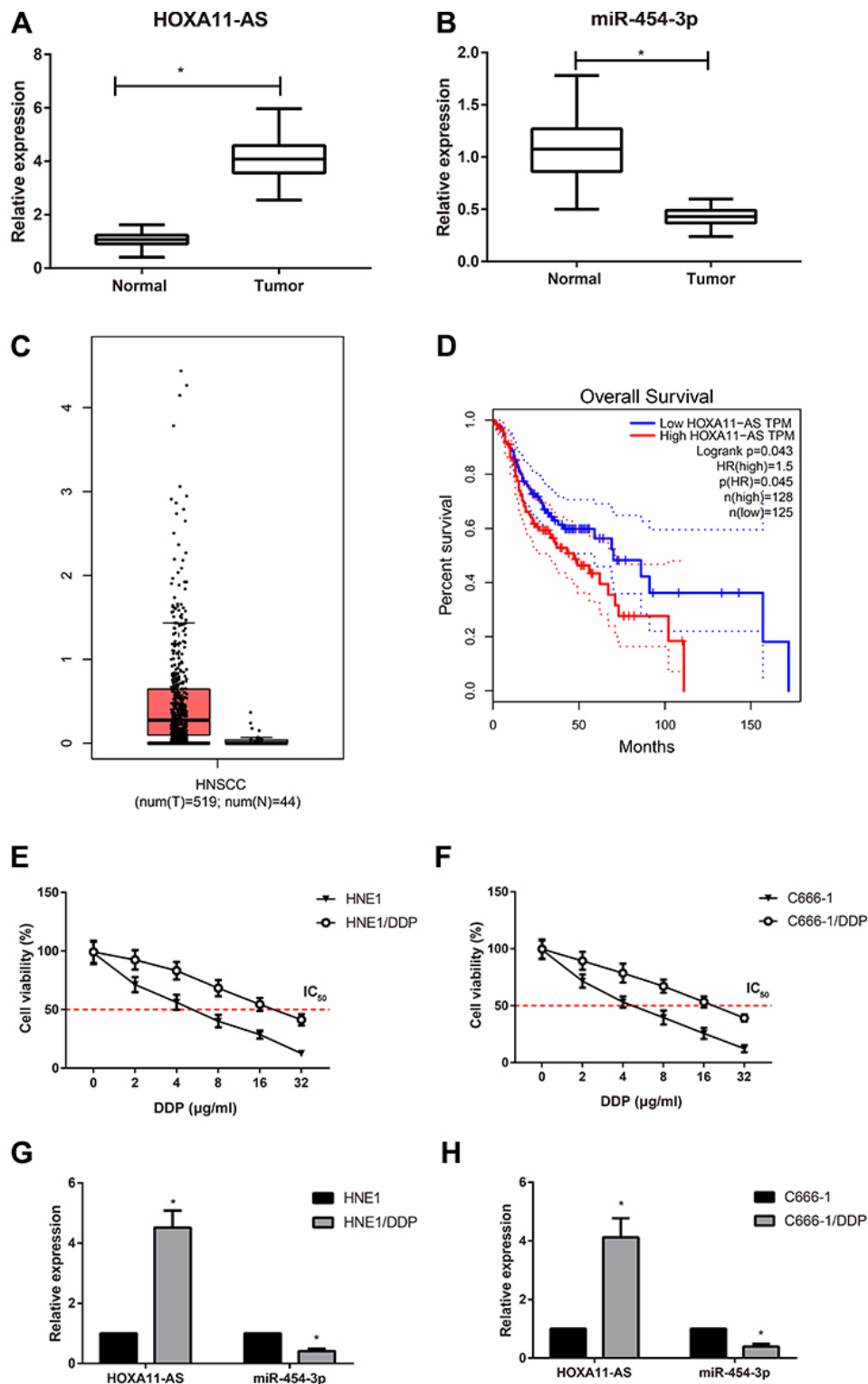
Fig. 1. Expression of HOXA11-AS and miR-454-3p in NPC tissues and drug-resistant cell lines. (A and B) Expression of HOXA11-AS (A) and miR-454-3p (B) in NPC tissues and tumor-adjacent normal tissues; *$P < 0.05$ vs the tumor-adjacent normal tissues. (C) The expression level of HOXA11-AS in HNSCC tissues and normal tissues in The Cancer Genome Atlas (TCGA) database was analyzed and is shown. (D) The survival curve was generated to analyze the correlation between HOXA11-AS expression and the overall survival of HNSCC patients based on TCGA dataset. (E and F) Viabilities and IC_{50} values of HNE1, C666-1, HNE1/DDP, and C666-1/DDP cells treated with DDP at varying concentration as assessed by MTT. (G and H) Expression of HOXA11-AS and miR-454-3p in NPC cells (HNE1, C666-1) and the corresponding cisplatin-resistant cells (HNE1/DDP, C666-1/DDP); *$P < 0.05$ vs HNE1 or C666-1 cells.

at dilutions of 1:500 at 4°C overnight: c-Met (ab51067; Abcam, UK), Akt (ab8805; Abcam), p-Akt (ab38449; Abcam), mTOR (ab2732; Abcam), p-mTOR (ab84400; Abcam), and β-actin (ab8226; Abcam). Later, the resulting immunoblots were further incubated with the corresponding secondary antibodies (Abcam) for 1 h, which was then terminated by rinsing the membrane in PBST three times, 5 min/wash. The final immunoblots were visualized with the Roche enhanced chemiluminescence (ECL) reagent (Millipore, USA). Finally, analysis of the band intensity was carried out with the ImageJ software for the target bands, with the intensity of β-actin used as the loading control.

Construction of the xenograft models in nude mice

BALB/c nude mice, aged between 6- and 8-week-old, were provided by the Shanghai Laboratory Animal Center of Chinese Academy of Sciences and divided into the following groups: control group (intraperitoneal injection of normal saline), DDP group (intraperitoneal injection of DDP), si-NC group (intratumoral injection of si-NC), si-HOXA11-AS group (intratumoral injection of si-HOXA11-AS), DDP + si-NC group and DDP + si-HOXA11-AS group, with 8 mice in each group. Following one week of adaptation, HNE1 cells in a logarithmic phase were collected and resuspended in PBS at density of 10^7 cells/ml. Then, HNE1 cells were injected subcutaneously in the axilla of the forelimbs of the nude mice, 0.2 ml/mouse. When the tumors reached approximately 300 mm^3, intratumoral injection of 100 µl of 250 nM si-NC/si-HOXA-11A manufactured with atelocollagen (daily) or intraperitoneal injection with DDP (25 mg/kg, twice a week) or a combination of si-NC/si-HOXA-11A and DDP were carried out (Wang et al., 2017). At the end of experiment, the mice were decapitated to remove the tumor for measuring the volume by using the following the formula: volume = (length/width^2)/2. In addition, the tumor was also weighed.

Statistical methods

The IBM SPSS Statistics 20.0 software (IBM, USA) was used for data analysis. Measurement data are presented as the mean ± standard deviation, and the difference between two groups was verified by the t-test, while the difference among groups was verified by the one-way ANOVA and Tukey's post hoc test. A $P < 0.05$ suggested that the difference had statistical significance.

RESULTS

Expression of HOXA11-AS and miR-454-3p in NPC tissues and drug-resistant cell lines

As shown in Figs. 1A and 1B, in comparison with the tumor-adjacent normal tissues, in NPC tissues HOXA11-AS was upregulated with the downregulation of miR-454-3p (all $P < 0.05$). For further confirmation, the expression level of HOXA11-AS in the neck squamous cell carcinoma (HNSCC) samples of The Cancer Genome Atlas (TCGA) database (https://cancergenome.nih.gov/) was analyzed, and the data showed that HOXA11-AS was expressed at a much higher level in HNSCC tissues than in normal tissues (Fig. 1C). A survival curve was generated to reveal the correlation between

HOXA11-AS expression and the overall survival of HNSCC patients by using the data from TCGA database. It could be observed that the overall survival rate in the HOXA11-AS high expression group was lower than that in the low expression group ($P < 0.05$; Fig. 1D). In addition, we used the MTT assay to examine the IC$_{50}$ values of parental NPC cells and the corresponding cisplatin-resistant cells to which DDP was added at varying concentrations. As expected, the IC$_{50}$ values of HNE1/DDP and C666-1/DDP cells were significantly higher than those of the HNE1 and C666-1 cells, respectively (Figs. 1E and 1F), suggesting that in response to DDP treatment, HNE1/DDP and C666-1/DDP cells were less sensitive than the HNE1 and C666-1 cells. We also found that HOXA11-AS was upregulated while miR-454-3p was downregulated in the HNE1/DDP and C666-1/DDP cells, compared to the HNE1 and C666-1 cells (all $P < 0.05$; Figs. 1G and 1H). All these findings indicated that HOXA11-AS was a poor prognostic factor for NPC patients and a potential biomarker for cisplatin resistance.

Targeting relationship among miR-454-3p, HOXA11-AS and c-Met

From the prediction websites of StarBase (http://starbase.sysu.edu.cn) and TargetScan (http://www.targetscan.org), we found the binding sites between miR-454-3p and HOXA11-AS (Fig. 2A) and between miR-454-3p and c-Met (Fig. 2B). We performed a luciferase reporter assay to verify that miR-454-3p could bind to HOXA11-AS and c-Met. Compared to the miR-NC group, cotransfection of HOXA11-AS-WT/c-Met-WT in the miR-454-3p mimic group obviously curbed the activity of luciferase, whereas the luciferase activity was enhanced by the miR-454-3p inhibitor ($P < 0.05$). However, HOXA11-AS-MUT/c-Met-MUT cotransfection with miR-454-3p mimic/miR-454-3p inhibitor/miR-NC led to no significant difference in the luciferase activity (all $P > 0.05$; Figs. 2C and 2D). We performed an RNA immunoprecipitation assay and confirmed that HOXA11-AS and miR-454-3p were enriched in Ago2 immunoprecipitates compared with control IgG immunoprecipitates from HNE1 and C666-1 cells (Fig. 2E). Moreover, RNA pull-down assays showed a higher expression of biotin-labeled miR-454-3p/c-Met in HOXA11-AS/miR-454-3p pull-down pellets than those of the beads alone and the negative control (Fig. 2F). Thus, the targeting relationships between HOXA11-AS and miR-454-3p and between miR-454-3p and c-Met were verified, which demonstrated that miR-454-3p could specifically bind to HOXA11-AS and c-Met.

Effect of HOXA11-AS on the cisplatin resistance of NPC cells

Compared to those in the control group, NPC cells (C666-1, HNE1) and their cisplatin-resistant clones (C666-1/DDP, HNE1/DDP) in the si-HOXA11-AS group showed clear downregulation of HOXA11-AS but upregulation of miR-454-3p (all $P < 0.05$; Fig. 3A), which was the opposite to the results of the miR-454-3p inhibitor group. After transfection, the IC$_{50}$ values of the parental cells (C666-1 and HNE1) and the cisplatin-resistant cells (C666-1/DDP and HNE1/DDP) were tested with the MTT assay (Fig. 3B). The viability and IC$_{50}$ val-

A

HOXA11-AS-WT   5' CAAATCTAATCGTGTATTGCACTG

hsa-miR-454-3p   3' TGGGATATTCGT - TATAACGTGAT

HOXA11-AS-MUT   5' CAAAACATTTGGTGATAACGTGAG

B

c-Met 3'UTR WT   5' UUGCUCUUGCCAAAAUUGCACUA

hsa-miR-454-3p   3' UGGGAUAUUCGUUAUAACGUGAU

c-Met 3'UTR MUT   5' UUGCUCUUGCCAAAUAACGUGAU

Fig. 2. HOXA11-AS upregulates c-Met by absorbing miR-454-3p. (A) The prediction website StarBase revealed the binding site between HOXA11-AS and miR-454-3p. (B) The prediction of TargetScan showed the binding site between miR-454-3p and c-Met. (C and D) Dual luciferase reporter gene assay verified the relationship between HOXA11-AS and miR-454-3p (C) and between miR-454-3p and c-Met (D); *$P < 0.05$ vs miR-NC group. (E) RIP experiment with an anti-Ago2 antibody, with IgG as a negative control or input from HNE1 and C666-1 cells using qRT-PCR as a positive control; *$P < 0.05$ vs anti-IgG group. (F) RNA pull-down assay were used to verify the target site between HOXA11-AS and miR-454-3p and between miR-454-3p and c-Met; *$P < 0.05$ vs beads group.

ue were lower in the si-HOXA11-AS, miR-454-3p mimic and si-c-Met groups in comparison with the control group, while those in the miR-454-3p inhibitor group showed the opposite changes (all $P < 0.05$). The cells in the si-HOXA11-AS + miR-454-3p inhibitor group demonstrated higher cell viabilities and IC_{50} values than those of the si-HOXA11-AS group (all P
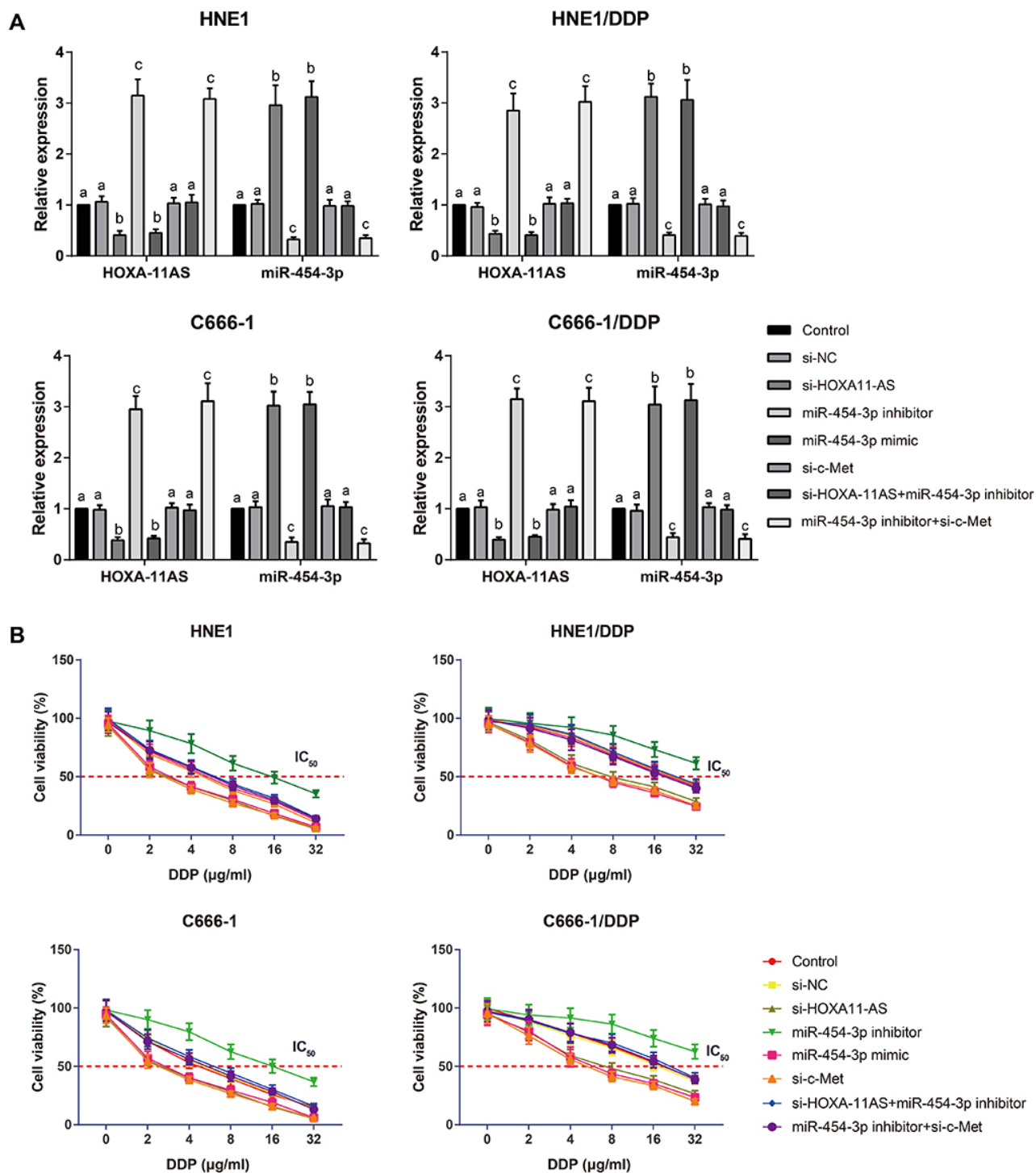
Fig. 3. Effect of HOXA11-AS on the cisplatin resistance of NPC cells. (A) Expression of HOXA11-AS and miR-454-3p in NPC parental cells (C666-1 and HNE1) and cisplatin-resistant cells (C666-1/DDP and HNE1/DDP) was assessed by qRT-PCR; different letters indicate the statistical significance among the groups, $P < 0.05$, and the same letters indicate no statistical significance among the groups, $P > 0.05$. (B) Cell viabilities and IC_{50} values of NPC parental cells (C666-1 and HNE1) and cisplatin-resistant cells (C666-1/DDP and HNE1/DDP) after treatment with DDP at varying concentrations, as assessed by MTT assay.

< 0.05). However, cells in the miR-454-3p inhibitor + si-c-Met group manifested lower viabilities and IC_{50} values than those in the miR-454-3p inhibitor group (all $P < 0.05$). Therefore,

we concluded that HOXA11-AS knockdown could improve the sensitivity of NPC cells to DDP by mediating miR-454-3p/c-Met.
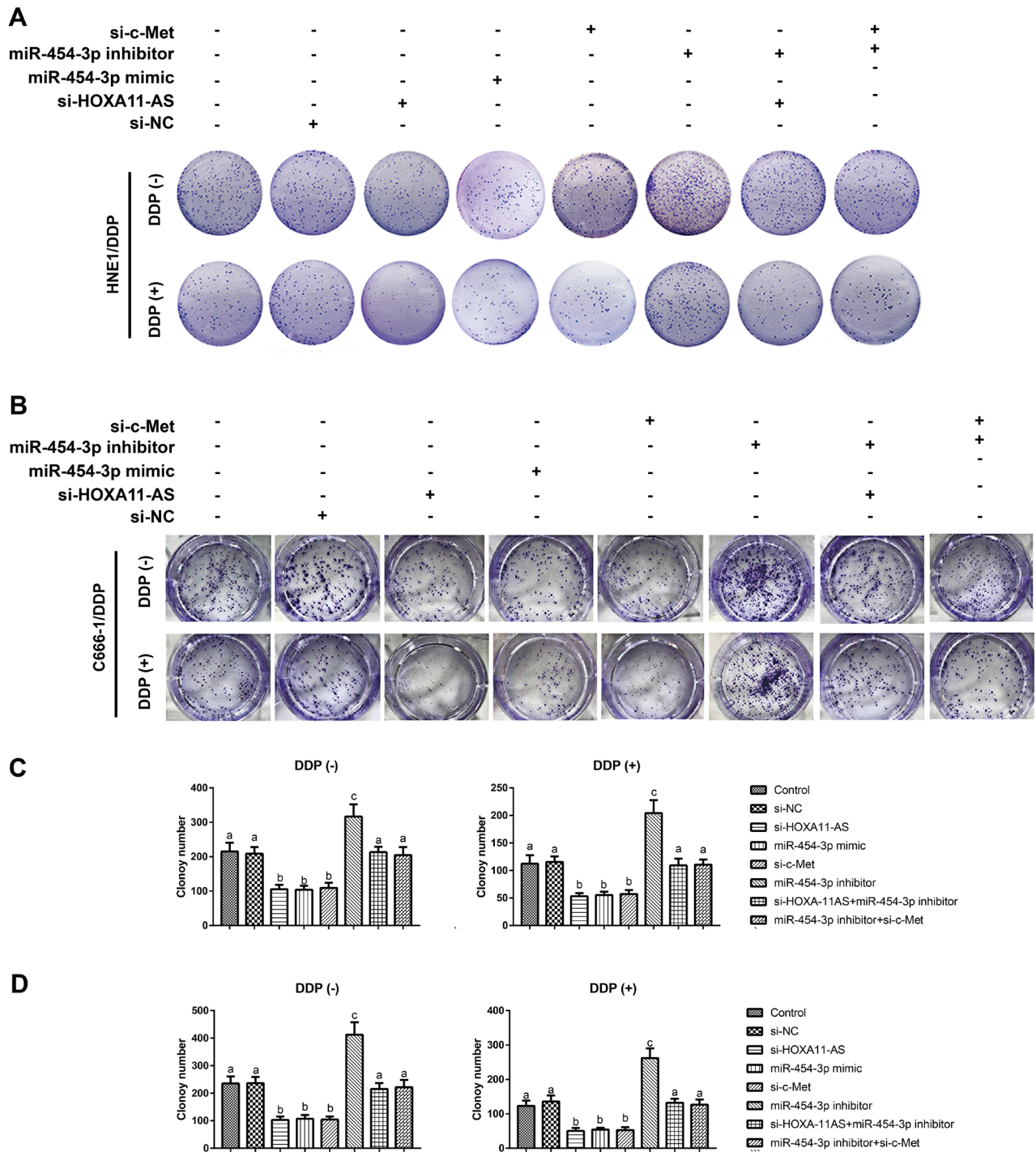
Fig. 4. Effect of HOXA11-AS on the clones of HNE1/DDP and C666-1/DDP cells treated with or without DDP. (A and B) Clones of HNE1/DDP (A) and C666-1/DDP (B) cells in different groups with or without treatment with DDP. (C and D) Comparison of the clones of HNE1/DDP (C) and C666-1/DDP (D) cells among the groups. Different letters indicate the statistical significance among the groups, $P <$ 0.05, and the same letters indicate no statistical significance among the groups, $P >$ 0.05.

Effect of HOXA11-AS on the clones of cisplatin-resistant NPC cells

We further investigated the effect of HOXA11-AS on cisplatin-resistant cells (C666-1/DDP and HNE1/DDP) that were treated with or without DDP. The colony formation assays re-vealed that the clones of C666-1/DDP and HNE1/DDP cells in the si-HOXA11-AS, miR-454-3p mimic and si-c-Met groups were much fewer than those in the control group, while those in the miR-454-3p inhibitor group showed a sharp in-crease (all $P <$ 0.05; Fig. 4). However, compared to the cells
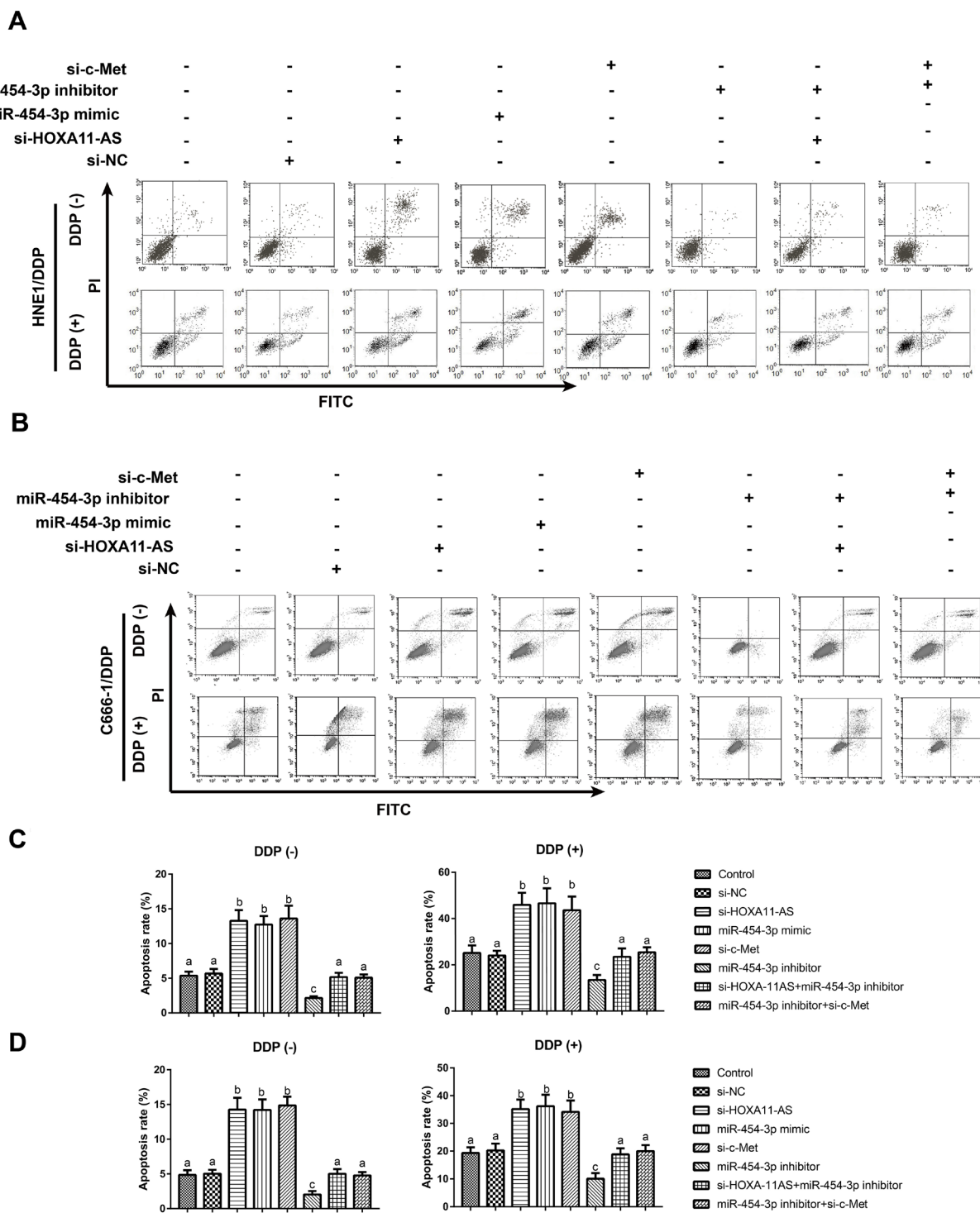
Fig. 5. Effect of HOXA11-AS on the apoptosis of HNE1/DDP and C666-1/DDP cells treated with or without DDP. (A and B) Flow cytometry results showed the apoptosis of HNE1/DPP (A) and C666-1/DDP (B) cells with and without treatment with DDP. (C and D) Comparison of the apoptotic rate of HNE1/DDP (C) and C666-1/DDP (D) cells among the groups. Different letters indicate the statistical significance among the groups, $P < 0.05$, and the same letters indicate no statistical significance among the groups, $P > 0.05$.

in the miR-454-3p inhibitor group, the cells in the miR-454-3p inhibitor + si-c-Met group showed fewer clones (all $P < 0.05$). Moreover, there were fewer clones in the DDP-treated cells than in those cells without DDP treatment, and the most clear decrease in the clones was identified in the cells cotreated with si-HOXA11-AS and DDP, indicating that the

inhibitory effect of si-HOXA11-AS was more obvious in the cells cotreated with DDP.

Effect of HOXA11-AS on the apoptosis of cisplatin-resistant NPC cells

Flow cytometry was performed to measure cell apoptosis in cisplatin-resistant cells (C666-1/DDP and HNE1/DDP), which were treated with or without DDP. As shown in Fig. 5, DDP treatment induced an obvious increase in the apoptotic rate in comparison with the DDP-free HNE1/DDP cells, and the most evident increase was found in HNE1/DDP and C666-1/DDP cells cotreated with si-HOXA11-AS, miR-454-3p mimic or si-c-Met and DDP. Compared to the control group, the HNE1/DDP cells in the si-HOXA11-AS, miR-454-3p mimic or si-c-Met groups showed a sharp increase in apoptotic rate, while those in the miR-454-3p inhibitor group showed a decline (all $P < 0.05$). Compared to that in the si-HOXA11-AS group, the apoptotic rate of the cells in the si-HOXA11-AS + miR-454-3p inhibitor group was obviously reduced (all $P < 0.05$), while in comparison with the miR-454-3p inhibitor group, the cells in the miR-454-3p inhibitor + si-c-Met showed a sharp increase in the apoptotic rate (all $P < 0.05$). All these results suggested that downregulation HOXA11-AS could promote DDP-induced apoptosis in cisplatin-resistant NPC cells.

Effect of HOXA11-AS on the c-Met/AKT/mTOR pathway in cisplatin-resistant NPC cells

To further determine whether HOXA11-AS regulated cisplatin resistance by affecting the c-Met/AKT/mTOR pathway, we examined the levels of the c-Met/AKT/mTOR pathway-related proteins with a Western blotting assay. Compared with that in the control group, c-Met, p-Akt/Akt and p-mTOR/mTOR expression in HNE1/DDP and C666-1/DDP cells from the si-HOXA11-AS, miR-454-3p mimic or si-c-Met groups was downregulated, while the miR-454-3p inhibitor group manifested the opposite changes (all $P < 0.05$; Fig. 6). Furthermore, compared to those in the si-HOXA11-AS group, c-Met, p-Akt/Akt and p-mTOR/mTOR in the si-HOXA-11AS + miR-454-3p inhibitor group were upregulated (all $P < 0.05$). Moreover, in comparison with the miR-454-3p inhibitor group, those proteins in the miR-454-3p inhibitor + si-c-Met group were obviously downregulated (all $P < 0.05$). Furthermore, c-Met, p-Akt/Akt and p-mTOR/mTOR in the DDP-treated HNE1/DDP and C666-1/DDP cells were lower than those in the DDP-free cells, while the downregulation of these proteins in the cells cotreated with si-HOXA11-AS and DDP was particularly evident. Taken together, these data suggested that the HOXA11-AS could mediate the c-Met/AKT/mTOR pathway in the cisplatin resistance of NPC cells by sponging miR-454-3p.

Effect of cotreatment of HOXA11-AS and DDP on the growth of subcutaneous xenografts in nude mice

To further verify these *in vitro* findings, we used an *in vivo* xenograft model. As shown in Fig. 7, the subcutaneous xenograft tumors in nude mice of the DDP group, si-HOXA11-AS group and DDP + si-HOXA11-AS group showed a significant decrease in growth and miR-454-3p expression compared to the control group, with sharp decreases in the volume and weight of the tumors, as well as the expression levels of HOXA11-AS and c-Met (all $P < 0.05$). In addition, the volume and weight of xenograft tumors in the DDP + si-HOXA11-AS group were much lower than those in the DDP group or si-HOXA11-AS group (all $P < 0.05$). The *in vitro* and *in vivo* results suggested that HOXA11-AS might promote the cisplatin resistance of NPC by modulating miR-454-3p/c-Met (Fig. 8).

DISCUSSION

First, it was demonstrated that HOXA11-AS was upregulated while miR-454-3p was downregulated in the NPC tissues and DDP-resistant HNE1/DDP cells. A meta-analysis performed by Lv et al. (2017) revealed the significant correlation of HOXA11-AS upregulation with the metastases and poor prognoses of various tumors. Recent studies have demonstrated that HOXA11-AS is upregulated in several cancers and contributed to the development of multiple types of cancers (PMID: 28791375). For instance, HOXA11-AS was shown to be elevated in lung adenocarcinoma tissues and lung cancer A540/DDP cells in the study of Zhang et al. (2019). However, the regulators involved in the disordered HOXA11-AS expression in cancer cells are not well known. Sun et al. (2016) demonstrated that HOXA11-AS overexpression in gastric cancer cells could be activated by E2F1, which can also promote lncRNA ERIC and ANRIL expression, and in addition, E2F1 was confirmed to be upregulated in various types of cancers according to previous studies (Han et al., 2003; Hung et al., 2012), including NPC (Tan et al., 2017). Here, we speculated that the overexpression of HOXA11-AS might be induced by E2F1 in various cancer cells.

However, there remains no adequate evidence suggesting the exact role of miR-454, a newly discovered miRNA in recent years. After assessing the expression of miRNAs in esophageal cancer, lower levels of miR-454 were observed compared to the surrounding normal tissues (Zhuang et al., 2013). Results from Niu et al. (2015) supported the downregulation of miR-454 in osteosarcoma, whereas overexpression weakened the proliferation and invasion of osteosarcoma cells via c-Met, and thus miR-454 may be a tumor suppressor. Furthermore, our results derived from the dual luciferase reporter assay showed that miR-454-3p was a target gene of HOXA11-AS and that c-Met was a target gene of miR-454-3p. Hence, we speculated that HOXA11-AS may play a role in the pathogenesis of DDP resistance of NPC by mediating the miR-454-3p/c-Met axis.

In this study, which used DDP-resistant HNE1/DDP cells, we found that silencing HOXA11-AS can inhibit the proliferation but facilitate the apoptosis of HNE1/DDP and C666-1/DDP cells in the absence of DDP, and by contrast, inhibiting miR-454-3p can reverse these changes. Accordingly, HOXA11-AS inhibition has been shown to suppress the growth and facilitate the apoptosis of glioma cells via upregulating miR-140-5p (Wu et al., 2014). Notably, HOXA11-AS, via competitively binding to miR-124, has been shown to promote the proliferation and invasion while suppressing the apoptosis of uveal melanoma cells, as reported by Lu et al. (2017). On the other hand, through upregulating miR-454-3p by knockdown of
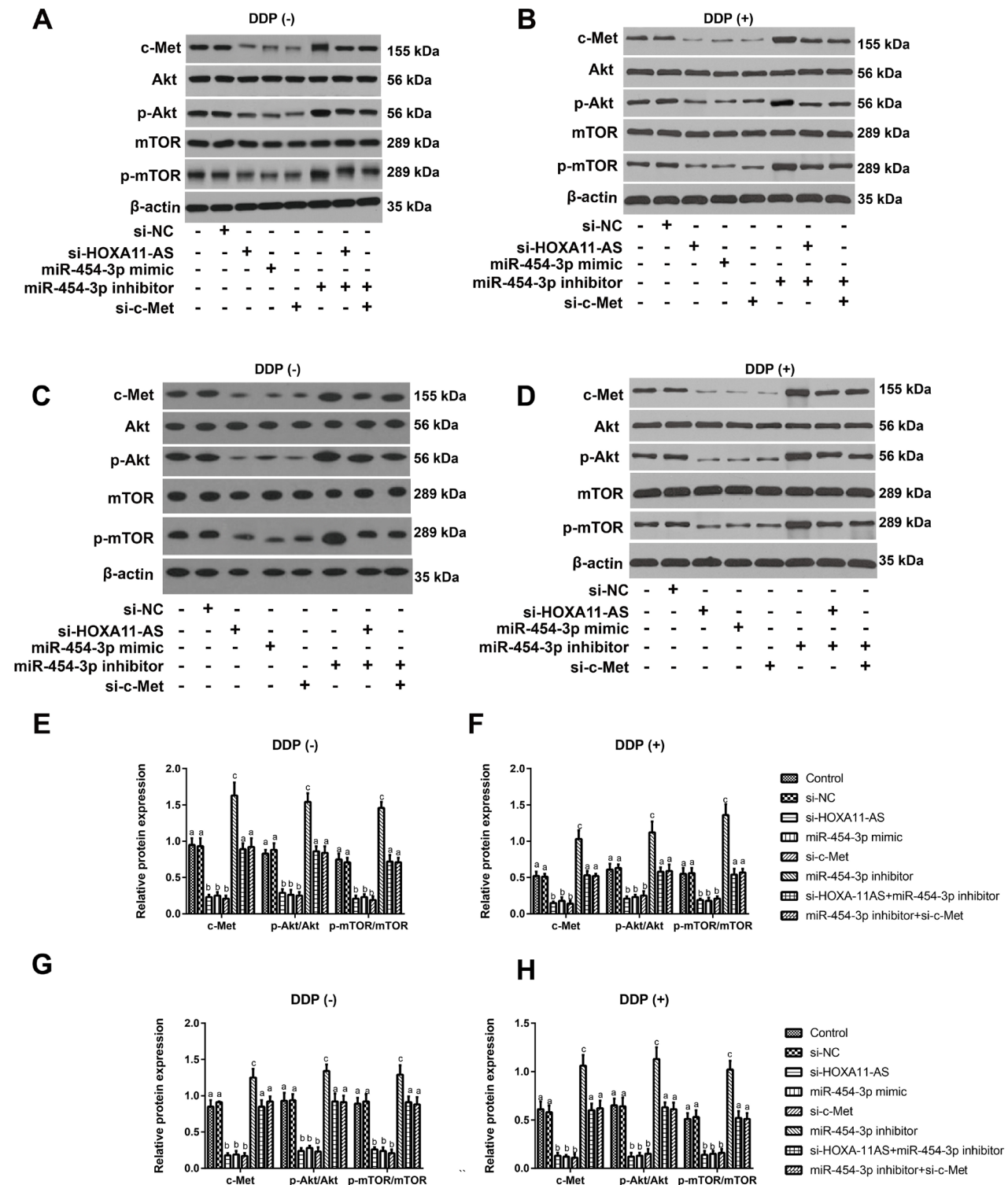
Fig. 6. Effect of HOXA11-AS on the c-Met/AKT/mTOR pathway in HNE1/DDP and C666-1/DDP cells. (A-D) Western blotting was used to assess the relative expression of proteins in the c-Met/AKT/mTOR pathway of HNE1/DDP (A and B) and C666-1/DDP (C and D) cells in the different groups without DDP treatment. (E-H) Western blotting was used to assess the relative expression of proteins in the c-Met/AKT/mTOR pathway of HNE1/DDP (E and F) and C666-1/DDP (G and H) cells in the different groups with DDP treatment. Different letters indicate the statistical significance among the groups, $P < 0.05$, and the same letters indicate no statistical significance among the groups, $P > 0.05$.
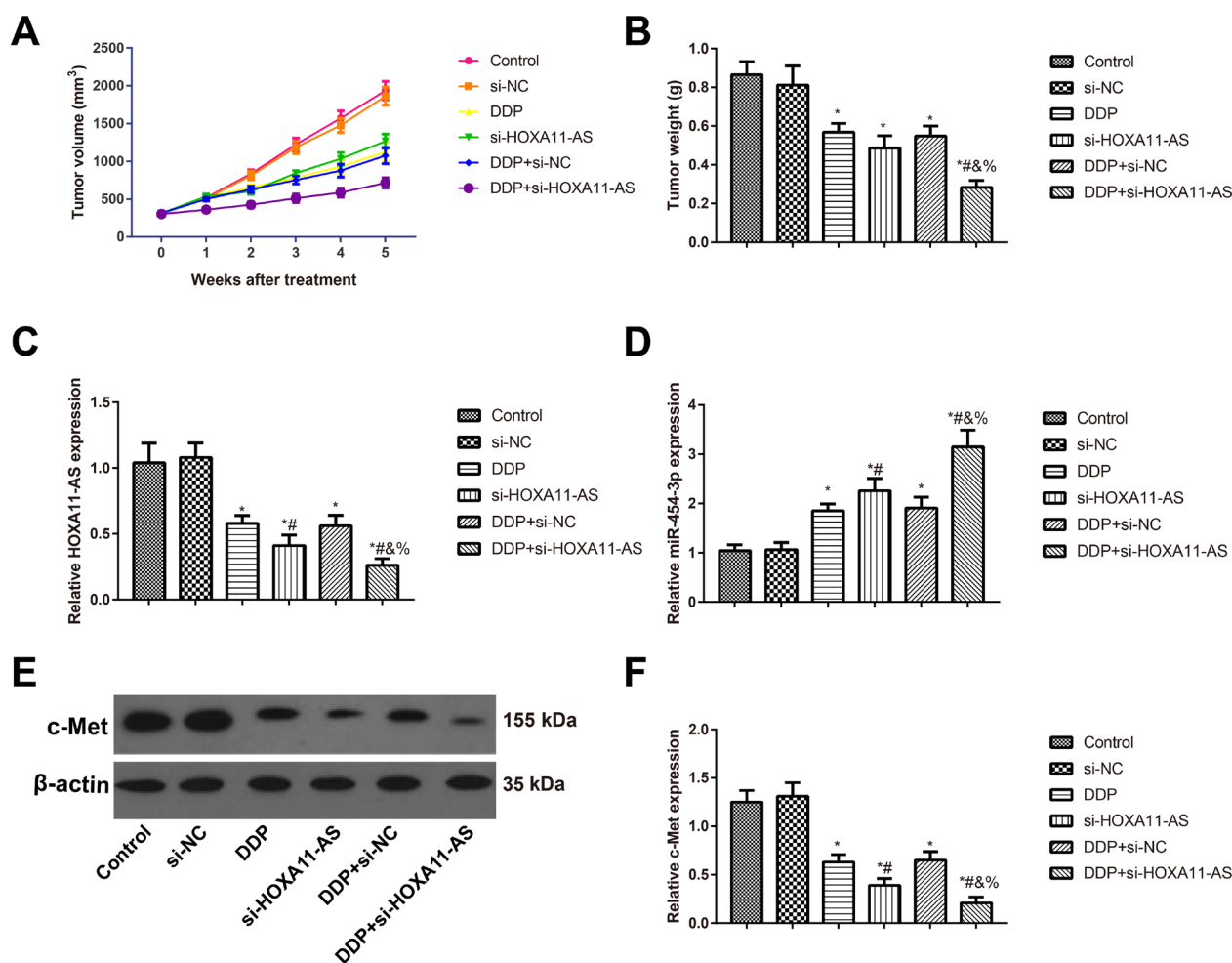
Fig. 7. The growth of subcutaneous xenografts in nude mice. (A) Growth curve of tumor growth in nude mice. (B) Comparison of the tumor weight in nude mice. (C and D) Expression of HOXA11-AS (C) and miR-454-3p (D) in nude mice as assessed by qRT-PCR. (E and F) Expression of c-Met in nude mice as assessed by Western blotting. *P < 0.05 vs the control group; #P < 0.05 vs the DDP group; &P < 0.05 vs the si-HOXA11-AS group; %P < 0.05 vs the DDP + si-NC group.
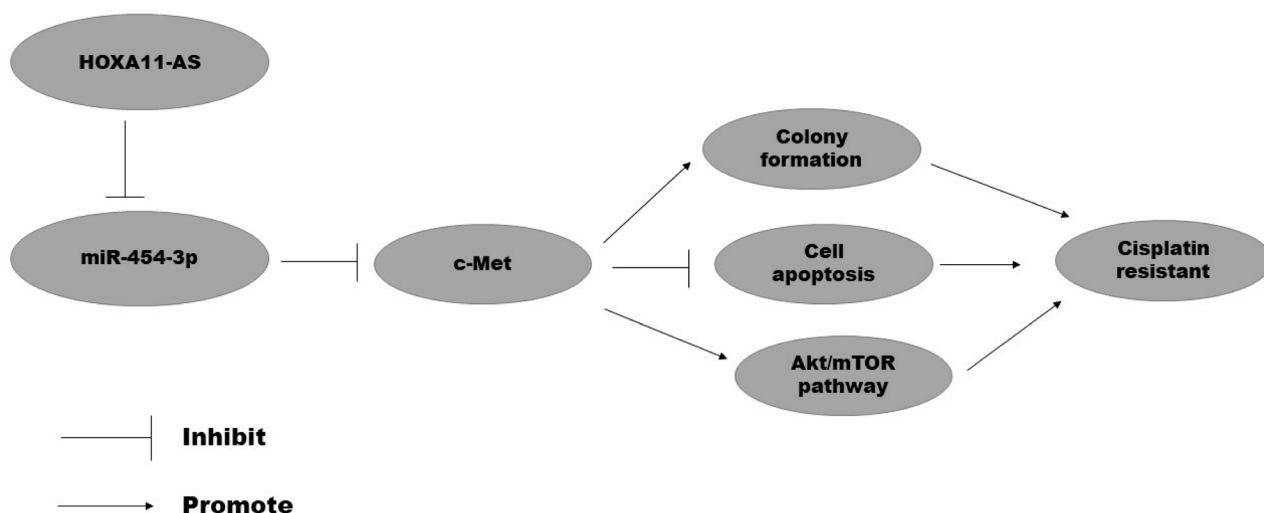

Fig. 8. The mechanism underlying the HOXA11-AS/miR-454-3p/c-Met axis in NPC.

HOTAIR, the growth of chondrosarcoma cells was suppressed with the reduced expression of STAT3 (Bao et al., 2017). Our subsequent experiments also demonstrated that silencing HOXA11-AS can increase the expression of miR-454-3p but that the miR-454-3p inhibitor can reverse this promoting effect of si-HOXA11-AS on cell growth. Thus, HOXA11-AS may serve as a ceRNA to regulate the expression of miR-454-3p, modulating the growth of NPC cells.

In addition, our findings showed that si-HOXA11-AS can reduce the viability of NPC cells and decrease the IC_{50} value after treatment with DDP at varying concentrations. In contrast, the miR-454-3p inhibitor can increase the viability and the IC_{50} value of cells. Similar to what was observed in DDP-resistant lung adenocarcinoma cells, Zhao et al. (2018) observed an enhanced HOXA11-AS, while the exogenous inhibition of HOXA11-AS could suppress cell proliferation and migration and increase its apoptosis by regulating the miR-454-3p/STAT3 axis. In addition, miR-454-3p can enhance the sensitivity of renal cancer cells to the radiotherapy by specifically inhibiting BTG1 (Wu et al., 2014). More importantly, we also found that in our DDP-treated HNE1/DDP and C666-1/DDP cells, silencing HOXA11-AS can significantly decrease the proliferation and increase the apoptosis of cells. Therefore, silencing HOXA11-AS can enhance the sensitivity of NPC cells to DDP by upregulating miR-454-3p and then reverse the resistance to DDP.

Last but not least, the activity of c-Met/AKT/mTOR, a downstream pathway of miR-454-3p, was assessed. The results showed that the transfection of si-HOXA11-AS in HNE1/DDP cells downregulates the expression of c-Met, p-Akt/Akt and p-mTOR/mTOR, while the transfection of miR-454-3p inhibitor results in the opposite changes and that si-c-Met transfection can also abolish the effect of the miR-454-3p inhibitor. Existing data have shown that the PI3K-AKT-mTOR pathway can promote the cell cycle and suppress cell apoptosis, demonstrating the intimate associations with metastasis and resistance to various anti-tumor drugs (Vadlakonda et al., 2013; Wang et al., 2014). c-Met can activate PI3K directly or indirectly, which may further induce the activation of downstream Akt, after which Akt can activate mTOR and MDM2 while suppressing BAD and GSK3β, thereby promoting cell growth and inducing apoptosis resistance (Dai et al., 2018; Hung et al., 2011). The study by Tang et al. (2017) revealed that the restricted c-Met/AKT/mTOR pathway may further inhibit multidrug resistance protein 1 (MDR1), thus enhancing the sensitivity of A549/DDP cells to DDP. Que et al. (2012) knocked out c-Met and found a decreased activity of the Akt/mTOR pathway with the increased apoptosis, thus reversing the resistance of myeloma cells to bortezomib. Considering the above results, si-HOXA11-AS may upregulate the expression of miR-454-3p, thus inhibiting the activity of c-Met/Akt/mTOR and regulating drug resistance or the expression of apoptosis-related proteins, finally affecting the sensitivity of NPC cells to DDP.

In conclusion, we found that HOXA11-AS was upregulated in NPC tissues and drug-resistant cells, while silencing HOXA11-AS might inhibit the activity of the c-Met/Akt/mTOR pathway by upregulating miR-454-3p, thus promoting cell apoptosis and increasing the sensitivity of DDP-resistant NPC cells to DDP. Hence, the results of this study may provide novel theoretical evidence for the treatment of DDP-resistant NPC patients.

AUTHOR CONTRIBUTIONS
F.J.L. and X.D.L. conceived and performed experiments, wrote the manuscript, and secured funding. L.Y.X. and S.Q.Z. performed experiments. F.J.L. and X.D.L. provided reagents. L.Y.X. and S.Q.Z. provided expertise and feedback.

CONFLICT OF INTEREST
The authors have no potential conflicts of interest to disclose.

ORCID
Feng-Jie Lin   https://orcid.org/0000-0002-8282-7612
Xian-Dong Lin   https://orcid.org/0000-0003-2403-2499
Lu-Ying Xu   https://orcid.org/0000-0003-3318-0864
Shi-Quan Zhu   https://orcid.org/0000-0003-1384-2234

REFERENCES

Bao, X., Ren, T., Huang, Y., Sun, K., Wang, S., Liu, K., Zheng, B., and Guo, W. (2017). Knockdown of long non-coding RNA HOTAIR increases miR-454-3p by targeting Stat3 and Atg12 to inhibit chondrosarcoma growth. Cell Death Dis. 8, e2605.

Bayne, K. (1996). Revised guide for the care and use of laboratory animals available. American Physiological Society. Physiologist 39, 199, 208-211.

Chen, Q.Y., Wen, Y.F., Guo, L., Liu, H., Huang, P.Y., Mo, H.Y., Li, N.W., Xiang, Y.Q., Luo, D.H., Qiu, F., et al. (2011). Concurrent chemoradiotherapy vs radiotherapy alone in stage II nasopharyngeal carcinoma: phase III randomized trial. J. Natl. Cancer Inst. 103, 1761-1770.

Colaco, R.J., Betts, G., Donne, A., Swindell, R., Yap, B.K., Sykes, A.J., Slevin, N.J., Homer, J.J., and Lee, L.W. (2013). Nasopharyngeal carcinoma: a retrospective review of demographics, treatment and patient outcome in a single centre. Clin. Oncol. (R. Coll. Radiol.) 25, 171-177.

Dai, C., Xie, Y., Zhuang, X., and Yuan, Z. (2018). MiR-206 inhibits epithelial ovarian cancer cells growth and invasion via blocking c-Met/AKT/mTOR signaling pathway. Biomed. Pharmacother. 104, 763-770.

Fang, B., Zhu, J., Wang, Y., Geng, F., and Li, G. (2015). MiR-454 inhibited cell proliferation of human glioblastoma cells by suppressing PDK1 expression. Biomed. Pharmacother. 75, 148-152.

Han, S., Liang, Y., Li, Y., and Du, W. (2016). Long noncoding RNA identification: comparing machine learning based tools for long noncoding transcripts discrimination. Biomed Res. Int. 2016, 8496165.

Han, S., Park, K., Bae, B.N., Kim, K.H., Kim, H.J., Kim, Y.D., and Kim, H.Y. (2003). E2F1 expression is related with the poor survival of lymph node-positive breast cancer patients treated with fluorouracil, doxorubicin and cyclophosphamide. Breast Cancer Res. Treat. 82, 11-16.

Hung, C.M., Kuo, D.H., Chou, C.H., Su, Y.C., Ho, C.T., and Way, T.D. (2011). Osthole suppresses hepatocyte growth factor (HGF)-induced epithelial-mesenchymal transition via repression of the c-Met/Akt/mTOR pathway in human breast cancer cells. J. Agric. Food Chem. 59, 9683-9690.

Hung, J.J., Hsueh, C.T., Chen, K.H., Hsu, W.H., and Wu, Y.C. (2012). Clinical significance of E2F1 protein expression in non-small cell lung cancer. Exp. Hematol. Oncol. 1, 18.

Jia, W.H. and Qin, H.D. (2012). Non-viral environmental risk factors for nasopharyngeal carcinoma: a systematic review. Semin. Cancer Biol. *22*, 117-126.

Kamran, S.C., Riaz, N., and Lee, N. (2015). Nasopharyngeal carcinoma. Surg. Oncol. Clin. N. Am. *24*, 547-561.

Kong, F., Cai, B., Lin, S., Zhang, J., Wang, Y., and Fu, Q. (2015). Assessment of radiotherapy combined with adjuvant chemotherapy in the treatment of patients with advanced nasopharyngeal carcinoma: a prospective study. J. BUON *20*, 206-211.

Li, T., Xu, C., Cai, B., Zhang, M., Gao, F., and Gan, J. (2016). Expression and clinicopathological significance of the lncRNA HOXA11-AS in colorectal cancer. Oncol. Lett. *12*, 4155-4160.

Li, Y., Zhang, S., Tang, Z., Chen, J., and Kong, W. (2011). Silencing of c-Met by RNA interference inhibits the survival, proliferation, and invasion of nasopharyngeal carcinoma cells. Tumour Biol. *32*, 1217-1224.

Liu, Z., Chen, Z., Fan, R., Jiang, B., Chen, X., Chen, Q., Nie, F., Lu, K., and Sun, M. (2017). Over-expressed long noncoding RNA HOXA11-AS promotes cell cycle progression and metastasis in gastric cancer. Mol. Cancer *16*, 82.

Lu, Q., Zhao, N., Zha, G., Wang, H., Tong, Q., and Xin, S. (2017). LncRNA HOXA11-AS exerts oncogenic functions by repressing p21 and miR-124 in uveal melanoma. DNA Cell Biol. *36*, 837-844.

Lv, W.P., Li, M.X., and Wang, L. (2017). Peroxiredoxin 1 inhibits lipopolysaccharide-induced oxidative stress in lung tissue by regulating P38/JNK signaling pathway. Eur. Rev. Med. Pharmacol. Sci. *21*, 1876-1883.

Niu, G., Li, B., Sun, J., and Sun, L. (2015). miR-454 is down-regulated in osteosarcomas and suppresses cell proliferation and invasion by directly targeting c-Met. Cell Prolif. *48*, 348-355.

Que, W., Chen, J., Chuang, M., and Jiang, D. (2012). Knockdown of c-Met enhances sensitivity to bortezomib in human multiple myeloma U266 cells via inhibiting Akt/mTOR activity. APMIS *120*, 195-203.

Song, J., Ye, A., Jiang, E., Yin, X., Chen, Z., Bai, G., Zhou, Y., and Liu, J. (2018). Reconstruction and analysis of the aberrant lncRNA-miRNA-mRNA network based on competitive endogenous RNA in CESC. J. Cell. Biochem. *119*, 6665-6673.

Sun, M., Nie, F., Wang, Y., Zhang, Z., Hou, J., He, D., Xie, M., Xu, L., De, W., Wang, Z., et al. (2016). LncRNA HOXA11-AS promotes proliferation and invasion of gastric cancer by scaffolding the chromatin modification factors PRC2, LSD1, and DNMT1. Cancer Res. *76*, 6299-6310.

Tan, Y., Wei, X., Zhang, W., Wang, X., Wang, K., Du, B., and Xiao, J. (2017). Resveratrol enhances the radiosensitivity of nasopharyngeal carcinoma cells by downregulating E2F1. Oncol. Rep. *37*, 1833-1841.

Tang, X.L., Yan, L., Zhu, L., Jiao, D.M., Chen, J., and Chen, Q.Y. (2017). Salvianolic acid A reverses cisplatin resistance in lung cancer A549 cells by

targeting c-met and attenuating Akt/mTOR pathway. J. Pharmacological Sciences *135*, 1-7.

Vadlakonda, L., Pasupuleti, M., and Pallu, R. (2013). Role of PI3K-AKT-mTOR and Wnt signaling pathways in transition of G1-S phase of cell cycle in cancer cells. Front. Oncol. *3*, 85.

Wang, Y., Cheng, N., and Luo, J. (2017). Downregulation of lncRNA ANRIL represses tumorigenicity and enhances cisplatin-induced cytotoxicity via regulating microRNA let-7a in nasopharyngeal carcinoma. J. Biochem. Mol. Toxicol. *31*, e21904.

Wang, Z., Huang, Y., and Zhang, J. (2014). Molecularly targeting the PI3K-Akt-mTOR pathway can sensitize cancer cells to radiotherapy and chemotherapy. Cell. Mol. Biol. Lett. *19*, 233-242.

Wu, X., Ding, N., Hu, W., He, J., Xu, S., Pei, H., Hua, J., Zhou, G., and Wang, J. (2014). Down-regulation of BTG1 by miR-454-3p enhances cellular radiosensitivity in renal carcinoma cells. Radiat. Oncol. *9*, 179.

Yu, J., Hong, J.F., Kang, J., Liao, L.H., and Li, C.D. (2017). Promotion of LncRNA HOXA11-AS on the proliferation of hepatocellular carcinoma by regulating the expression of LATS1. Eur. Rev. Med. Pharmacol. Sci. *21*, 3402-3411.

Zhang, L., Chen, Q.Y., Liu, H., Tang, L.Q., and Mai, H.Q. (2013). Emerging treatment options for nasopharyngeal carcinoma. Drug Des. Devel. Ther. *7*, 37-52.

Zhang, Y., Chen, W.J., Gan, T.Q., Zhang, X.L., Xie, Z.C., Ye, Z.H., Deng, Y., Wang, Z.F., Cai, K.T., Li, S.K., et al. (2017). Clinical significance and effect of lncRNA HOXA11-AS in NSCLC: a study based on bioinformatics, in vitro and in vivo verification. Sci. Rep. *7*, 5567.

Zhang, Y., He, R.Q., Dang, Y.W., Zhang, X.L., Wang, X., Huang, S.N., Huang, W.T., Jiang, M.T., Gan, X.N., Xie, Y., et al. (2016). Comprehensive analysis of the long noncoding RNA HOXA11-AS gene interaction regulatory network in NSCLC cells. Cancer Cell Int. *16*, 89.

Zhang, Y., Yuan, Y., Li, Y., Zhang, P., Chen, P., and Sun, S. (2019). An inverse interaction between HOXA11 and HOXA11-AS is associated with cisplatin resistance in lung adenocarcinoma. Epigenetics *14*, 949-960.

Zhao, X., Li, X., Zhou, L., Ni, J., Yan, W., Ma, R., Wu, J., Feng, J., and Chen, P. (2018). LncRNA HOXA11-AS drives cisplatin resistance of human LUAD cells via modulating miR-454-3p/Stat3. Cancer Sci. *109*, 3068-3079.

Zhou, L., Qu, Y.M., Zhao, X.M., and Yue, Z.D. (2016). Involvement of miR-454 overexpression in the poor prognosis of hepatocellular carcinoma. Eur. Rev. Med. Pharmacol. Sci. *20*, 825-829.

Zhuang, R., Rao, J.N., Zou, T., Liu, L., Xiao, L., Cao, S., Hansraj, N.Z., Gorospe, M., and Wang, J.Y. (2013). miR-195 competes with HuR to modulate stim1 mRNA stability and regulate cell migration. Nucleic Acids Res. *41*, 7905-7919.